

# Discovery of hydroxytyrosol as thioredoxin reductase 1 inhibitor to induce apoptosis and G<sub>1</sub>/S cell cycle arrest in human colorectal cancer cells via ROS generation

SHENG-PENG ZHANG<sup>1\*</sup>, JI ZHOU<sup>2\*</sup>, QING-ZHU FAN<sup>1</sup>, XIAO-MEI LV<sup>1</sup>, TIAN WANG<sup>3</sup>,  
FAN WANG<sup>3</sup>, YANG CHEN<sup>3</sup>, SEN-YAN HONG<sup>3</sup>, XIAO-PING LIU<sup>1</sup>, BING-SONG XU<sup>3</sup>,  
LEI HU<sup>3</sup>, CHAO ZHANG<sup>1</sup> and YE-MING ZHANG<sup>3</sup>

<sup>1</sup>Center of Drug Screening and Evaluation, <sup>2</sup>Center for Reproductive Medicine, The First Affiliated Hospital,  
<sup>3</sup>School of Pharmacy, Wannan Medical College, Wuhu, Anhui 241000, P.R. China

Received August 22, 2020; Accepted April 30, 2021

DOI: 10.3892/etm.2021.10261

**Abstract.** Colorectal cancer (CRC) is one of the most common cancer types and a leading cause of cancer-associated mortality in China. Increased thioredoxin reductase 1 (TrxR1) levels have been previously identified as possible target for CRC. The present study revealed that the natural product hydroxytyrosol (HT), which exhibits a polyphenol scaffold, is a potent inhibitor of TrxR1. Inhibition of TrxR1 was indicated to result in accumulation of reactive oxygen species, inhibit proliferation and induce apoptosis and G<sub>1</sub>/S cell cycle arrest of CRC cells. Using a C-terminal mutant TrxR1 enzyme activity assay, TrxR1 RNA interference assay and HT binding model assay, the present study demonstrated the core character of the selenocysteine residue in the interaction between HT and TrxR1. HT can serve as polyphenol scaffold to develop novel TrxR1 inhibitors for CRC treatment in the future.

## Introduction

Colorectal cancer (CRC) is the second most common type of cancer and the leading cause of cancer-associated mortality in China (1). It is associated with obesity, type 2 diabetes and chronic inflammatory disease (2). Although progress has been achieved in the traditional treatment of CRC, it remains one

of the most lethal malignancies globally due to the limited therapeutics, high recurrence rate and poor prognosis (3). Thus, identification of safer and more effective treatments for CRC is required.

Mammalian thioredoxin (Trx) reductase 1 (TrxR1) is a selenoprotein that functions to maintain redox homeostasis in cells via transferring electrons from NADPH to its substrate Trx (4,5). Both Trx and TrxR1 are reported to be upregulated in CRC cells and have been associated with poor prognosis and resistance to chemotherapy (6-9). Increasing evidence has suggested that TrxR1 is involved in multiple steps of tumorigenesis (10-14). Therefore, TrxR1 is a potential target for anticancer drug development for CRC.

Natural products and their synthetic analogues are a major source of therapeutic agents and have been used for centuries to treat a variety of human ailments (15,16). Hydroxytyrosol (HT) is a major bioactive component of olive leaves and oil with a polyphenol scaffold, which has been demonstrated to exhibit a wide variety of pharmacological activities, including anti-inflammatory (17), neuroprotective (18), immunomodulatory (19) and antimicrobial activities (20-22). HT has been indicated to exhibit anticancer properties due to its important antiproliferative and pro-apoptotic effects in different types of cancer cells, including colon cancer cells. This effect could be mediated via numerous signaling pathways, for example, inhibition of ERK1/2 (23), antagonization of the G-protein-coupled estrogen receptor (24), dysregulated expression of catalase (25-27) and inhibition of the Akt, NF- $\kappa$ B, STAT3 and EGFR signaling pathways (28-30). Notably, the majority of the cellular actions of HT are associated with the induction of reactive oxygen species (ROS) production in colon cancer cells (25-27). In addition, the polyphenol scaffold has been revealed to be a useful scaffold for the TrxR1 inhibitor development (31). Therefore, the molecular mechanisms of ROS induction by HT require further elucidation.

The present study reported that HT is a potent inhibitor of TrxR1 with the ability to inhibit both the recombinant and the cellular TrxR1 in colon cancer cells. Inhibition of TrxR1 by HT induced accumulation of ROS, promoted apoptosis and inhibited proliferation. Silencing of TrxR1 expression by RNA

---

*Correspondence to:* Dr Chao Zhang, Center of Drug Screening and Evaluation, Wannan Medical College, 22 Wenchang West Road, Wuhu, Anhui 241000, P.R. China  
E-mail: zhangchao@wnmc.edu.cn

Mr. Ye-Ming Zhang, School of Pharmacy, Wannan Medical College, 22 Wenchang West Road, Wuhu, Anhui 241000, P.R. China  
E-mail: 547195050@qq.com

\*Contributed equally

**Key words:** thioredoxin, hydroxytyrosol, oxidative stress, apoptosis, antitumor

interference enhanced the cytotoxicity and the TrxR1 inhibitory activity of HT, supporting that TrxR1 is involved in the cellular actions of HT. The discovery of TrxR1 targeting by HT provided insight into the pharmacological activity of HT and indicated ability of HT to induce cellular ROS. Thus, HT could potentially be used for the development of novel TrxR1 inhibitors. Together with evidence from previously published data (26), HT could be developed as a clinical treatment for patients with CRC.

## Materials and methods

**Materials.** The natural compound library (cat. no. L6000) was purchased from Shanghai Topscience Co., Ltd. DMSO, NADPH, insulin, 5,5'-dithiobis-2-nitrobenzoic acid (DTNB), EDTA and recombinant human Trx (expressed in *E. coli*) were purchased from Sigma-Aldrich (Merck KGaA). Cell Counting Kit-8 (CCK-8; cat. no. CK04) and caspase-3 activity detection kit (cat. no. C551) were purchased from Dojindo Molecular Technologies, Inc. Rabbit polyclonal anti-TrxR1 antibody (cat. no. 11117-1-AP) was purchased from Wuhan Sanying Biotechnology. Mouse monoclonal anti-GAPDH antibody (cat. no. MA515738), HRP-conjugated goat anti-rabbit (cat. no. 31460) and goat anti-mouse (cat. no. 31430) IgG (H+L) secondary antibodies were purchased from Thermo Fisher Scientific, Inc. ROS assay kit (cat. no. S0033) and RIPA lysis buffer (cat. no. P0013B) were purchased from Beyotime Institute of Biotechnology. FITC Annexin V Apoptosis Detection Kit I (cat. no. 556547) was purchased from BD Biosciences. Protease and phosphatase inhibitor cocktail (cat. no. 78440) and Pierce BCA Protein Assay Kit (cat. no. 23225) were purchased from Thermo Fisher Scientific, Inc.

**Cell culture.** All human cell lines were purchased from American Type Culture Collection (ATCC). The normal colon epithelial cell line FHC was cultured in DMEM/F12 medium (cat. no. 30-2006; ATCC) with a final concentration of 25 mM HEPES, 10 ng/ml cholera toxin (cat. no. C8052; Sigma-Aldrich; Merck KGaA), 0.005 mg/ml insulin (cat. no. 91077C; Sigma-Aldrich; Merck KGaA), 0.005 mg/ml transferrin (cat. no. T8158; Sigma-Aldrich; Merck KGaA), 100 ng/ml hydrocortisone (cat. no. HY-N0583; MedChemExpress), 20 ng/ml human recombinant EGF (cat. no. PHG0311; Thermo Fisher Scientific, Inc.) and 10% (v/v) FBS (cat. no. 10099141C; Thermo Fisher Scientific, Inc.). HCT-8 and HCT-116 cells were cultured in RPMI-1640 medium (Thermo Fisher Scientific, Inc.) supplemented with 10% (v/v) FBS; SW620 cells were cultured in Leibovitz's L-15 medium (Thermo Fisher Scientific, Inc.) supplemented with 10% (v/v) FBS. All cells except SW620 (cultured with no CO<sub>2</sub> at 37°C) were maintained in a humidified atmosphere with 5% CO<sub>2</sub> at 37°C. All treated cells were incubated at 37°C in the following experiments.

**Recombinant protein production.** Plasmid pET-TRSter was a gift from Elias Arnér (cat. no. 78865; Addgene, Inc.; <http://n2t.net/addgene:78865>) (32), and recombinant rat TrxR1 protein (TrxR-wt) was expressed in *E. coli* BL21 (DE3) strain. TrxR-wt protein was purified by 2',5'-ADP-Sepharose column (Cytiva) with protein purification system (AKTA pure 25; Cytiva).

Recombinant mutant human TrxR1 (residues 1-496; lack of core sites Cys497 and Sec498 residues in the redox active center of the C-terminal) with an N-terminal His tag (pET-28a-TrxR1-ΔC) was expressed in the *E. coli* BL21 (DE3) strain and purified by immobilized metal affinity chromatography with protein purification system (AKTA pure 25; Cytiva).

Plasmid pET-28a-TrxR1-ΔC was constructed by cloning DNA encoding human TrxR1 protein (residues 1-496) into pET28a vector (cat. no. 69864; Sigma-Aldrich; Merck KGaA) using *EcoRI* and *NcoI* restriction sites. Recombinant rat TrxR1 (TrxR-wt) and mutant human TrxR1 enzyme activity were measured via DTNB assay and calculated using the following formula:  $\text{TrxR1 U/mg protein} = (\Delta A_{\text{pro}} - \Delta A_{\text{blank}}) / (\epsilon \times d) \times 10^9 \times V_{\text{total}} / (C_{\text{pr}} \times V_{\text{pro}}) / T$ .  $\Delta A_{\text{pro}}$  was the absorbance of wells with TrxR1 protein,  $\Delta A_{\text{blank}}$  was the absorbance of wells without TrxR1 protein,  $\epsilon$  was the molar extinction coefficient,  $d$  was the optical path length of the 96-well plate,  $V_{\text{total}}$  was the total reaction volume (unit,  $\mu\text{l}$ ),  $C_{\text{pr}}$  was the concentration of TrxR1 protein (unit,  $\mu\text{l}/\mu\text{g}$ ),  $V_{\text{pro}}$  was the TrxR1 protein volume in the reaction (unit,  $\mu\text{l}$ ),  $T$  was the reaction time (unit, min) and  $U$  was the enzyme units generating 1 nM 2-nitro-5-thiobenzoate per mg TrxR1 protein per min. The activity of recombinant rat TrxR1 was 511 U/mg protein, while that of recombinant mutant TrxR1 was 23 U/mg protein.

**TrxR1 enzyme assay.** TrxR1 activity was determined at room temperature using a microplate reader. The NADPH-reduced recombinant rat TrxR1 (100 nM) or mutant human TrxR1 (1  $\mu\text{M}$ ) was incubated with different concentrations of HT for 1 h at room temperature (the final volume of the mixture was 50  $\mu\text{l}$ ) in a 96-well plate. A mixture in Tris-EDTA buffer (50 mM Tris-HCl pH 7.5; 1 mM EDTA; 50  $\mu\text{l}$ ) containing DTNB and NADPH was added (final concentration 2 mM and 200  $\mu\text{M}$ , respectively), and the linear increase in absorbance (AB) at 412 nm during the initial 3 min was recorded. The same amount of DMSO (0.1%; v/v) was added to the control experiments, and the TrxR1 inhibitory rate was calculated using the following formula:  $\text{TrxR1 Inhibitory rate} = [1 - (\text{AB value of test at 3 min} - \text{AB value of test at 0 min}) / (\text{AB value of control at 3 min} - \text{AB value of control at 0 min})] \times 100\%$ .

**Cellular TrxR1 activity assay.** After HCT-116 or SW620 cells were treated with different concentrations (2-fold dilution for 11 concentrations starting at 100  $\mu\text{M}$ ) of HT for 24 h, the cells were harvested and washed twice with PBS. Total cellular proteins were extracted using RIPA buffer for 30 min on ice and quantified using the BCA method. TrxR1 activity in cell lysates was measured via the endpoint insulin reduction assay. Briefly, the cell extract containing 20  $\mu\text{g}$  total protein was incubated in a final reaction volume of 50  $\mu\text{l}$  containing 100 mM Tris-HCl (pH 7.6), 0.3 mM insulin, 660  $\mu\text{M}$  NADPH, 3 mM EDTA and 1.3  $\mu\text{M}$  recombinant human Trx for 30 min at 37°C. The reaction was terminated by adding 200  $\mu\text{l}$  of 1 mM DTNB in 6 M guanidine hydrochloride, pH 8.0 at 25°C for 5 min. A blank sample, containing everything except Trx, was treated in the same manner. The AB at 412 nm was measured, and the blank value was subtracted from the corresponding absorbance value of the sample. The same amount of DMSO was added to the control experiments and the TrxR1 inhibitory rate

was calculated using the following formula:  $\text{TrxR1 Inhibitory rate} = [1 - (\text{AB value of sample} - \text{AB value of blank}) / (\text{AB value of control} - \text{AB value of blank})] \times 100\%$ .

**Cell proliferation assay.** The effect of drug treatments on cell proliferation was quantified using a CCK-8 assay in HCT-116, SW620, HCT-8 and FHC cell lines. A total of 5,000 cells per well were seeded in 96-well plates overnight and then treated with HT (2-fold dilution for 12 concentrations starting at 200  $\mu\text{M}$ ). Complete culture medium without drug was added to the blank wells. Control cells were treated with DMSO only. After culture for 24 h, 10  $\mu\text{L}$  CCK-8 was added to each well and cells were incubated at 37°C for 4 h. Subsequently, the plate was gently shaken at 25°C for 10 min. The AB at 450 nm was measured using a Cytation 5 microplate reader (BioTek Instruments, Inc.), and the cell cytotoxicity inhibition rate was calculated using the following formula:  $\text{Growth inhibition rate} = (\text{AB value of control} - \text{AB value of test}) / (\text{AB value of control} - \text{AB value of blank}) \times 100\%$ . Cells were also pretreated with 3 mM N-acetylcysteine (NAC) for 2 h prior to HT exposure, followed by analysis of the effect of NAC on the inhibitory effect of HT on cell proliferation.

**Imaging TrxR1 activity in HCT-116 and SW620 cells by TRFS-green.** Cells were treated with the indicated concentrations (5, 10 and 20  $\mu\text{M}$  for HCT-116 cells; 15, 30 and 60  $\mu\text{M}$  for SW620 cells) of HT for 24 h followed by treatment with TRFS-green (10  $\mu\text{M}$ ) (33) for 4 h. Phase contrast and fluorescence images were captured using fluorescence microscopy (EVOS FL). A total of 10 cells were randomly selected, and the fluorescence intensity in individual cells was quantified using ImageJ software (version 1.8; National Institutes of Health).

**Western blotting.** HCT-116 or SW620 cells were treated with HT at the indicated concentrations for 24 h (5, 10 and 20  $\mu\text{M}$  for HCT-116 cells; 15, 30 and 60  $\mu\text{M}$  for SW620 cells). Cells were lysed with RIPA lysis buffer. Protein quantification was performed using a BCA Protein Assay Kit, following which equal quantities of proteins (20  $\mu\text{g}/\text{lane}$ ) were separated via a 4-20% gradient SDS-PAGE gel and transferred onto a PVDF membrane. The membranes were blocked with 5% BSA (cat. no. V900933; Sigma-Aldrich; Merck KGaA) at room temperature for 2 h. TrxR1 antibody was used at a 1:2,000 dilution and GAPDH antibody was used at a 1:5,000 dilution in 5% BSA and the membranes were incubated at 4°C overnight. Following three washes in TBS/0.1% Tween 20, the membranes were probed with the aforementioned HRP-conjugated secondary antibodies at a 10,000-fold dilution in 5% BSA. Following six washes with TBS/0.1% Tween 20, the immune complexes were incubated with SuperSignal™ West Pico PLUS reagent (cat. no. 34577; Thermo Fisher Scientific, Inc.) and detected using the ChemiDoc™ Touch Imaging system (Bio-Rad Laboratories, Inc.). The intensity of the resulting bands on the membranes was calculated and normalized to GAPDH in each sample using ImageJ software (version 1.8; National Institutes of Health). For the detection of the knock-down efficiency of TrxR1, cells were pre-transfected with small interfering (si)TrxR1 for 60 h prior to lysis as described below.

**Apoptosis assay.** HCT-116 and SW620 cells were plated in six-well plates at an initial density of  $2.4 \times 10^5$  cells/well for 8 h in complete RPMI-1640 medium. Cells were divided into the following three treatment groups: i) DMSO (Control); ii) HT treatment (5, 10 and 20  $\mu\text{M}$  in HCT-116 cells; 15, 30 and 60  $\mu\text{M}$  in SW620 cells); and iii) a combination of HT and 3 mM NAC. Cells were starved in serum-free RPMI-1640 medium for 16 h, except that groups with NAC treatment were pretreated with 3 mM NAC for 2 h after starvation in serum-free medium for 14 h, followed by HT treatment for 24 h. Cells were harvested, washed twice with PBS (Thermo Fisher Scientific, Inc.), evaluated for apoptosis using FITC Annexin V Apoptosis Detection kit I according to the manufacturer's protocol and analyzed using Novocyte® flow cytometer with NovoExpress® version 1.2.4 software (ACEA Bioscience, Inc.).

**Caspase-3 activity assay.** This experiment was performed using the aforementioned caspase-3 activity detection kit according to the manufacturer's instructions. Briefly, HCT-116 cells were treated with the indicated concentrations of HT for 24 h. Subsequently, the cells were collected and lysed with RIPA lysis buffer for 15 min at 0°C, using the Bradford method to quantify the protein content. A total of 50  $\mu\text{g}$  protein were incubated with 10  $\mu\text{l}$  Ac-DEVD-pNA substrate and 40  $\mu\text{l}$  assay buffer at 37°C for 2 h in a final volume of 100  $\mu\text{l}$ . The absorbance at 405 nm was read on a microplate reader.

**Cell cycle assay.** HCT-116 and SW620 cells were seeded in a six-well plate at an initial density of  $2.4 \times 10^5$  cells/well and allowed to attach overnight in complete culture medium. Cells were divided into three treatment groups, as aforementioned in the apoptosis assay. Cells were starved in serum-free culture medium for 24 h, except that groups with NAC treatment were pretreated with 3 mM NAC for 2 h after starvation in serum-free medium for 22 h, followed by HT treatment for 12 h. Cells were harvested, washed twice with PBS, evaluated for cell cycle using the cell cycle assay kit (cat. no. BB-4104; BestBio) and analyzed using the Novocyte® flow cytometer with NovoExpress® version 1.2.4 software (ACEA Bioscience, Inc.).

**RNA interference analysis.** TrxR1 siRNA and a scramble non-targeting negative control siRNA (siNC) were purchased from Biomics Biotechnologies Co., Ltd. The siRNAs (final concentration, 50 nM) were transfected into cells using Lipofectamine® 3000 reagent (Thermo Fisher Scientific, Inc.) according to the manufacturer's instructions. The siRNA sequences were as follows: siTrxR1 sense, 5'-GCAUCAAGCAGCUUUGUUAAdTdT-3', siTrxR1 antisense, 5'-UAACAAAGCUGCUUGAUGCdTdT-3'; siNC sense, 5'-UUCUCCGAA CGUGUCACGUdTdT-3', siNC antisense, 5'-ACGUGACAC GUUCGAGAAAdTdT-3'. For the loss-of-function analysis, HCT-116 or SW620 cells were pre-transfected with siNC or siTrxR1 for 36 h prior to HT exposure, followed by the same process as in CCK-8 assay, cellular TrxR1 activity assay and TRFS-green imaging.

**Measurement of ROS generation.** Cellular ROS content was measured by flow cytometry and fluorescence microscopy for quantitative and qualitative evaluation. HCT-116 or SW620 cells were plated in six-well plates at a density of

$2.0 \times 10^5$  cells/well and allowed to attach overnight, and were then exposed to the indicated concentrations of HT for 4 h (5, 10 and 20  $\mu\text{M}$  for HCT-116 cells; 15, 30 and 60  $\mu\text{M}$  for SW620 cells). Cells were stained with 10  $\mu\text{M}$  2',7'-dichlorofluorescein diacetate (DCFH-DA; Beyotime Institute of Biotechnology) at 37°C for 30 min and then washed three times in serum-free culture medium. For flow cytometry, cells were collected, and fluorescence was analyzed at excitation and emission wavelengths of 488 and 525 nm, respectively, using the Novocyte® flow cytometer with NovoExpress® version 1.2.4 software (ACEA Bioscience, Inc.). The mean value of DCFH-DA fluorescence intensity was utilized for quantitative analysis. For fluorescence microscopy, cell images were captured using the EVOS FL Imaging System (Thermo Fisher Scientific, Inc.).

*Time course of HT activity assay.* For the time course assay, HCT-116 cells were cultured as aforementioned, and then exposed to 20  $\mu\text{M}$  HT for 16, 24 and 32 h followed by apoptosis assay, western blotting and TRFS-green imaging. For ROS generation measurement, cells were exposed to 20  $\mu\text{M}$  HT for 2, 4 and 6 h, followed by DCFH-DA fluorescence assay.

*Docking of HT to the TrxR1 structural model.* To further study the interaction between HT and TrxR1, a docking study was implemented by Molecular Operating Environment (MOE) version 2019.0102 (<https://www.chemcomp.com/index.htm>). The crystal structure of human TrxR1 (Protein Data Bank code 2ZZ0, chain A; <https://www.rcsb.org/structure/2ZZ0>) was used for the present docking study. The central coordination of the dock pocket was examined by Site Finder through MOE software, which was calculated by selecting residues Cys497 and Sec498. The default parameters were used for implementing the docking simulation.

*Statistical analysis.* All statistical analyses were performed using GraphPad Prism software version 9.0 (GraphPad Software, Inc.). Results are presented as the mean  $\pm$  standard deviation of at least three independent experiments for each group. Statistical differences for the datasets of apoptosis rate and cell cycle distribution were analyzed via two-way ANOVA, while other data sets consisting of  $>2$  groups were analyzed via one-way ANOVA, followed by Tukey-Kramer post hoc test for multiple comparisons if significance was determined. For data not conforming to a normal distribution, Kruskal-Wallis test was used for multiple comparisons.  $P < 0.05$  was considered to indicate a statistically significant difference.

## Results

*HT inhibits TrxR1 activity in vitro.* To screen potent inhibitors of TrxR1, a TrxR1 activity assay was performed with a natural compound library against the recombinant TrxR1 enzyme (4,457 compounds; purity,  $>90\%$ ). Out of these, eight compounds were indicated to exhibit TrxR1 enzyme inhibitory activity. Among them, HT (the structure of this compound is depicted in Fig. 1A) could effectively inhibit TrxR1-wt activity with an  $\text{IC}_{50} \sim 1 \mu\text{M}$ , but exhibited little effect on the TrxR1- $\Delta\text{C}$  enzyme, a mutant TrxR1 lacking Cys497 and Sec498 residue in the C-terminal of wt TrxR1 (Fig. 1B). These results indicated that the Sec residue in TrxR1 was associated

with the inhibition of TrxR1 by HT. The inhibition of cellular TrxR1 by HT was further confirmed using an insulin reduction assay and image-based live cell TrxR1 activity assay. As illustrated in Fig. 1C, treating HCT-116 cells with HT led to a notable inhibition of cellular TrxR1 activity, with an  $\text{IC}_{50}$  of  $\sim 21.84 \mu\text{M}$ . By measuring and quantifying the fluorescence signal of this probe, a decrease in TrxR1 activity in living HCT-116 cells treated with HT compared with control cells was confirmed (Fig. 1D and E). Both assays produced consistent results revealing a dose-dependent inhibition of TrxR1 by HT in HCT-116 cells. Taken together, these data demonstrated that HT is a potent TrxR1 inhibitor.

*HT treatment inhibits proliferation and induces accumulation of ROS.* The antiproliferative effects of HT were tested in cultured human CRC cells (HCT-116, SW620 and HCT-8 cells) and normal colon cells (FHC cells). It was observed that HT treatment preferentially suppressed proliferation of all three CRC cells tested in a dose-dependent manner (Fig. 2A). By contrast, HT treatment exhibited a weak effect on normal FHC cells compared with that on cancer cells. In addition, the TrxR1 expression levels of HCT-116 cells were the highest among all three CRC cell lines, while those of SW620 cells were the lowest (data not shown). Thus, HCT-116 and SW620 cell lines were selected to investigate the cellular function of HT. TrxR1 protein levels were significantly decreased after the cells were treated with HT for 24 h (Fig. 2B), indicating that the decreased TrxR1 protein expression levels may account for the decreased TrxR1 enzyme activity after HT treatment.

The major function of TrxR1 is to maintain Trx in a reduced state and prevent oxidative stress (34). Having confirmed that HT was a potent TrxR1 inhibitor, the levels of ROS were then determined in HCT-116 and SW620 cells. ROS levels in the two cell lines were assessed by flow cytometry and cell imaging using the redox-sensitive fluorescent probe DCFH-DA. As presented in Fig. 2C and D, treatment with HT for 4 h significantly increased ROS levels in a dose-dependent manner, indicating that HT exhibited the ability to induce cellular ROS accumulation. Taken together, these results suggested that HT treatment inhibited proliferation and promoted accumulation of ROS in CRC cells.

*HT treatment induces apoptosis and G<sub>1</sub>/S cell cycle arrest in HCT-116 and SW620 cells.* Since excess ROS levels could be cytotoxic (35), apoptosis was examined using Annexin V/PI double staining assay. A significant increase in the percentage of apoptotic cells was detected after HT treatment for 24 h in HCT-116 and SW620 cells (Fig. 3A and B). Similar results were observed in the caspase-3 activity assay, where a significant concentration-dependent activation of caspase-3 was observed after a 24-h treatment with HT in HCT-116 cells (Fig. 3C).

By contrast, NAC inhibited the apoptosis-inducing effect of HT treatment in HCT-116 and SW620 cells, and the effects of ROS induction on cell cycle arrest were also determined. Cells were treated with various concentrations of HT with or without NAC for 24 h. The results in Fig. 4A and B indicated that HT treatment significantly induced G<sub>1</sub>/S cell cycle arrest in HCT-116 and SW620 cells. NAC significantly inhibited the

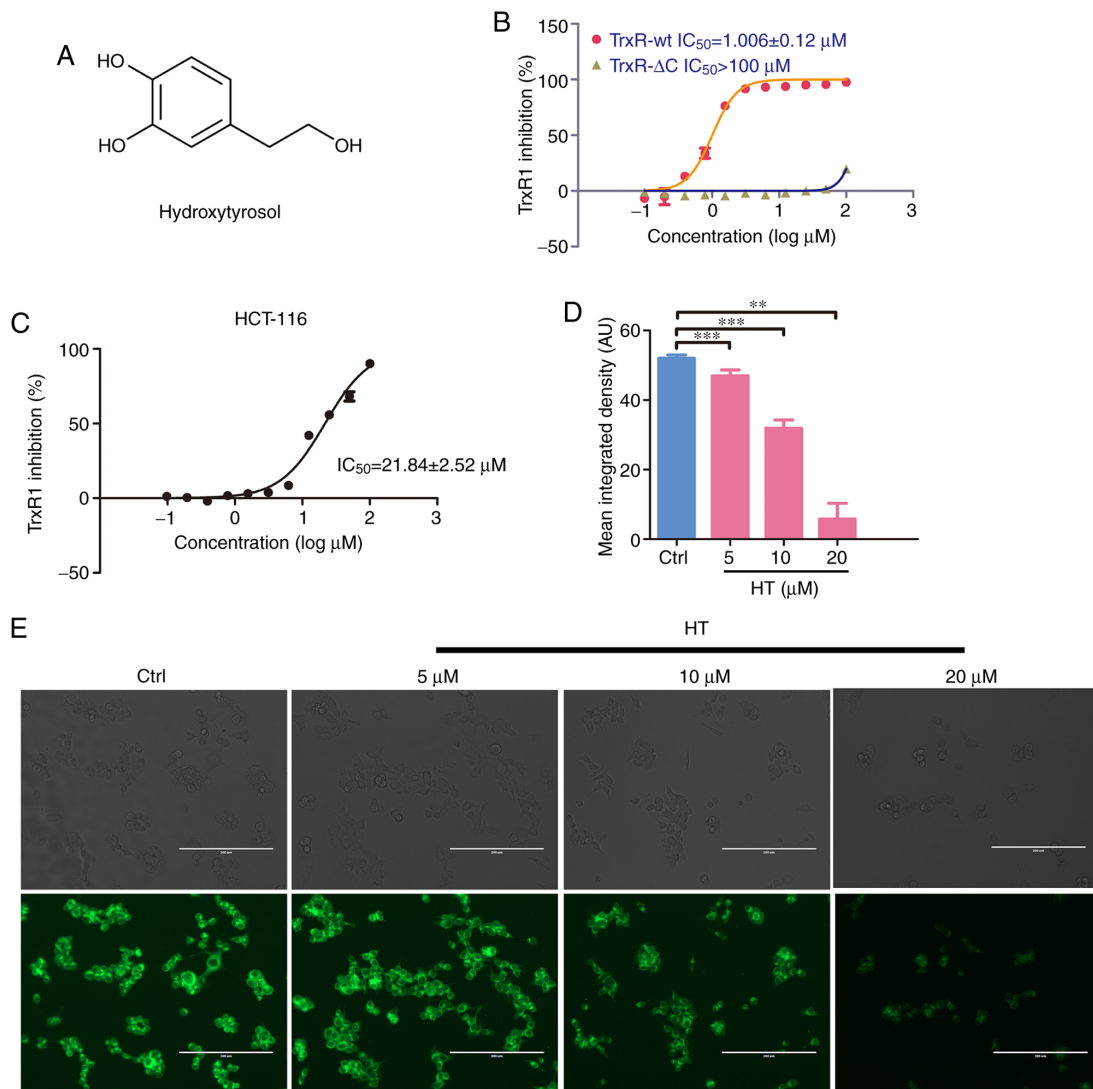


Figure 1. Inhibition of TrxR by HT. (A) Chemical structure of HT. (B) Inhibition of TrxR-wt and TrxR-ΔC by HT. (C) Inhibition of TrxR enzyme activity in HCT-116 cells. (D) Quantification of the mean fluorescence intensity in individual groups stained with TRFS-green. (E) HCT-116 cells were incubated with the indicated concentrations of HT, and then the TrxR probe TRFS-green was loaded. Phase-contrast (top) and fluorescence (bottom) images were captured using fluorescence microscopy. DMSO was used as the negative control. Scale bars, 200 μm. \*\* $P < 0.01$  and \*\*\* $P < 0.005$ . TrxR, thioredoxin reductase; HT, hydroxytyrosol; wt, wild-type; ΔC, C-terminal deletion mutant; AU, absorbance units.

cell cycle arrest effect of HT treatment in both cell lines. In addition, NAC pre-treatment inhibited the antiproliferative effect of HT in HCT-116 and SW620 cells (Fig. 4C). These results demonstrated that HT treatment promoted apoptosis and  $G_1/S$  cell cycle arrest in CRC cells via its effect on ROS generation.

*Antitumor effect of HT treatment is associated with its interaction with TrxR1.* To investigate the underlying structural mechanism of HT binding to the TrxR1 protein, a molecular simulation of the HT-TrxR1 complex was performed using docking software. As presented in Fig. 5A, HT was indicated to form hydrogen bonds with Sec498, Cys497, Gln494 and Trp407 residues of the C-terminal active site of the redox center of TrxR1 (34,36-39). Thus, the proposed reaction mechanism for HT is the simultaneous inhibition of the adjacent C-terminal active site residues of TrxR1, which is expected to effectively suppress TrxR1 activity. This mechanism is consistent with the difference in the HT-mediated

TrxR1 inhibition of the TrxR-wt and TrxR-ΔC enzymes, as the TrxR-ΔC enzyme lacks the core site Sec498 and Cys497 residues for HT binding.

As HT inhibition of both the recombinant and the cellular TrxR1 enzyme was demonstrated (Fig. 1), the physiological significance of TrxR1 inhibition in the cellular actions of HT was further investigated. TrxR1 expression levels were reduced in HCT-116 and SW620 cells following transfection of an siRNA specifically targeting TrxR1, and the knockdown efficiency was validated (Fig. 5B). As presented in Fig. 5C, HT exhibited a higher antiproliferative effect in siNC-transfected cells compared with siTrxR1-transfected cells. Knocking down TrxR1 was helpful for better characterizing the TrxR1 inhibitory activity of HT, which was further confirmed via the Trx-mediated insulin reduction assay (Fig. 5B) and the image-based assay using the specific TrxR1 probe TRFS-green in HCT-116 and SW620 cells (Fig. 5D and E). Taken together, the data supported the conclusion that the antiproliferative effect of HT was associated with its interaction with TrxR1.

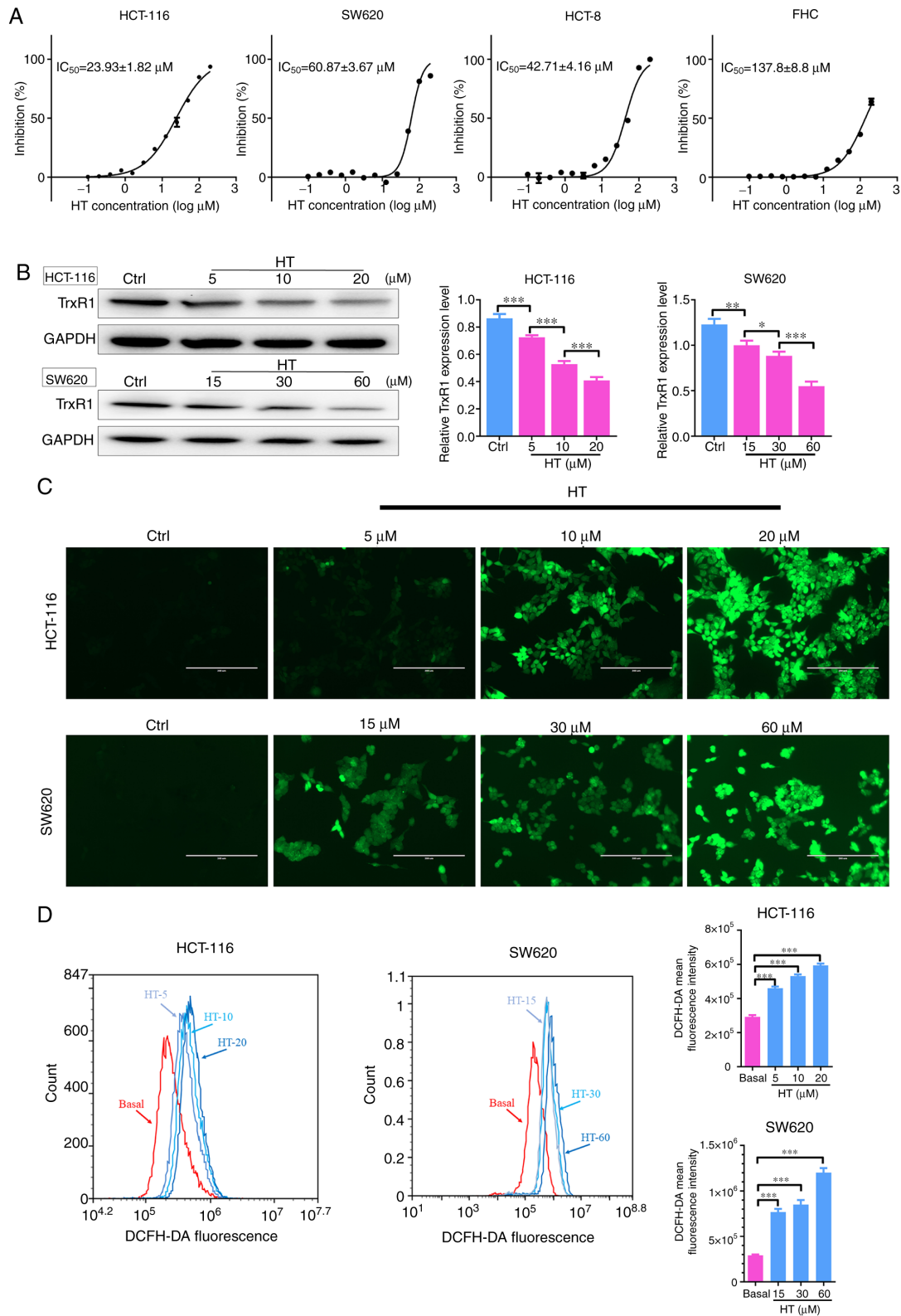


Figure 2. Effects of HT treatment on cell proliferation, TrxR expression levels and ROS accumulation. (A) Effect of increasing doses of HT on the proliferation of human colorectal cancer cell lines (HCT-116, HCT-8, SW620) and the normal FHC cell line. (B) Cells were treated with the indicated concentrations of HT for 24 h, and cell extracts were prepared and analyzed via western blotting with an antibody against TrxR1. TrxR1 expression levels were quantified and normalized to GAPDH. Intracellular ROS generation was induced by increasing doses of HT, and it was detected via staining with 10  $\mu M$  DCFH-DA and examined via (C) fluorescence microscopy and (D) flow cytometry in HCT-116 and SW620 cells. DCFH-DA mean fluorescence intensity was quantified by flow cytometry. DMSO was used as the negative control. Scale bars, 200  $\mu m$ . \* $P < 0.05$ , \*\* $P < 0.01$  and \*\*\* $P < 0.005$ . TrxR, thioredoxin reductase; HT, hydroxytyrosol; ROS, reactive oxygen species; DCFH-DA, 2',7'-dichlorofluorescein diacetate.

In addition, a time course assay was performed to further confirm the association between the antitumor effects and the

TrxR1 inhibitory activity of HT. As illustrated in Fig. 6A, C and F, HT treatment could reduce the expression level and

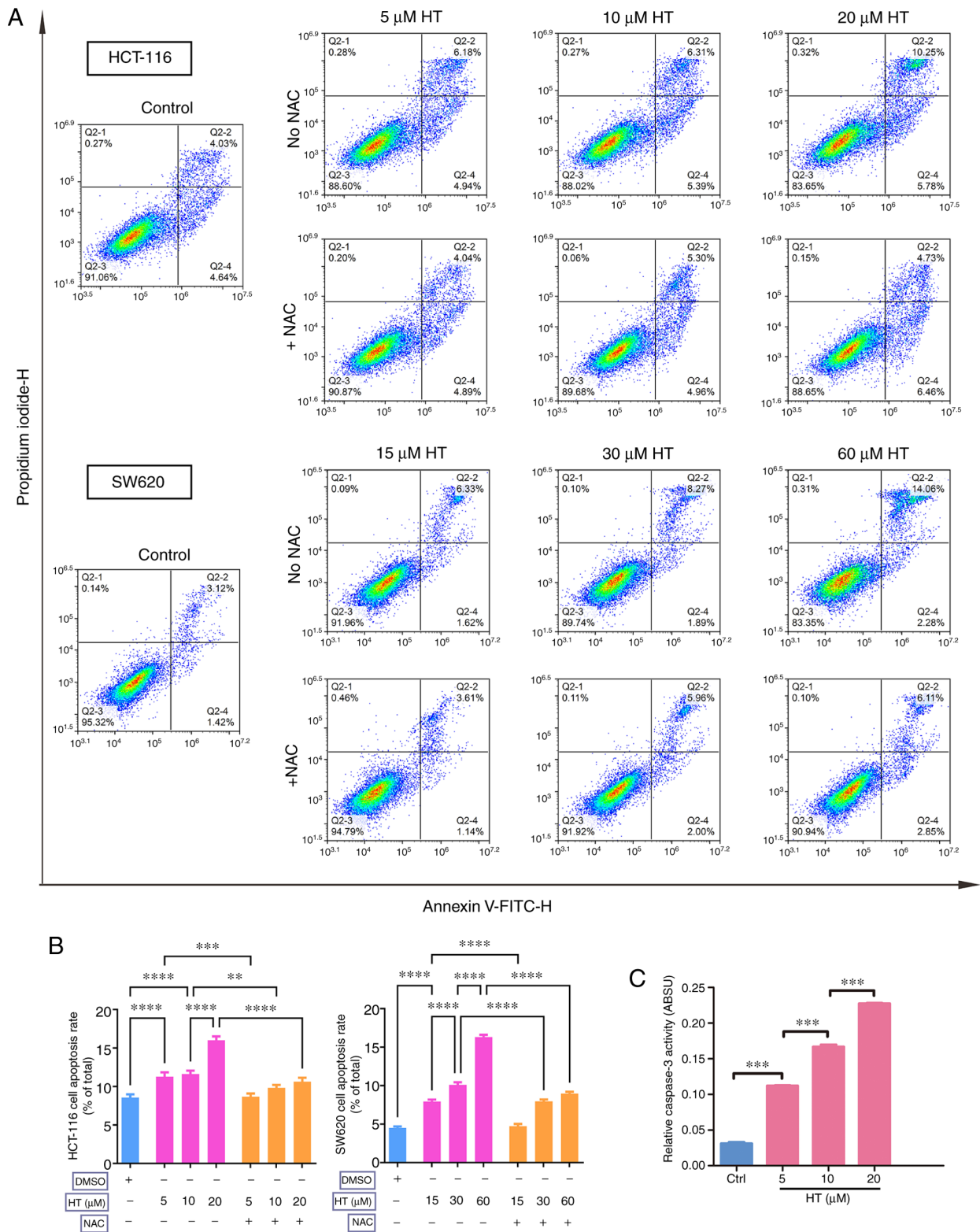


Figure 3. Induction of apoptosis by HT. (A) Analysis of apoptosis by Annexin V/propidium iodide double-staining assay. HCT-116 and SW620 cells were treated with HT alone or combined with 3mM NAC at the indicated concentrations for 24 h. (B) The percentage of cell apoptosis was quantified and cells in Q2-2 and Q2-4 were considered apoptotic. (C) Activation of caspase-3 by HT in HCT-116 cells after incubation with the indicated concentrations of HT for 24 h. DMSO was used as the negative control. \*\*P<0.01, \*\*\*P<0.005 and \*\*\*\*P<0.001. HT, hydroxytyrosol; NAC, N-acetylcysteine; ABSU, absorbance units.

activity of TrxR1 protein in a time course-dependent manner. However, HT treatment also induced ROS accumulation and apoptosis in a time course-dependent manner (Fig. 6B, D, E and G). These results partly demonstrated the antitumor effect of HT and revealed its association with TrxR1.

**Discussion**

HT has been indicated to induce ROS generation in cancer cells (26). To the best of our knowledge, the mechanism responsible for ROS induction by HT remains unclear. The results of

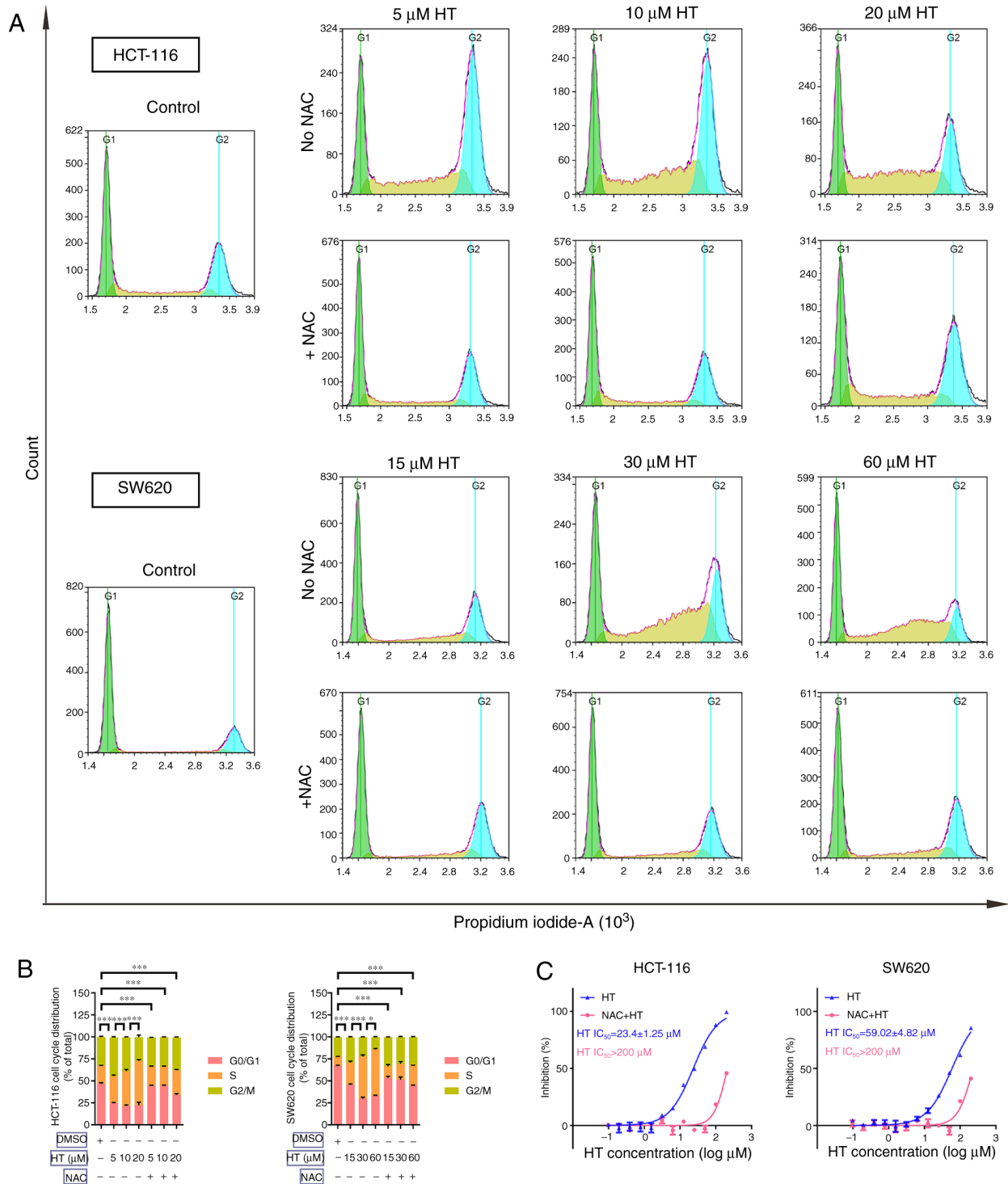


Figure 4. Induction of cell cycle arrest by HT. (A) Analysis of cell cycle arrest by propidium iodide staining assay. HCT-116 and SW620 cells were treated with HT alone or combined with 3 mM NAC at the indicated concentrations for 12 h. (B) Cell cycle distribution was examined by flow cytometry and quantified. (C) NAC antagonized the antiproliferative effect of HT in HCT-116 and SW620 cells. Cells were treated with increasing doses of HT alone or combined with 3 mM NAC for 24 h. DMSO was used as the negative control. \* $P < 0.05$  and \*\*\* $P < 0.005$ . NAC, N-acetylcysteine; HT, hydroxytyrosol.

the present study demonstrated that HT treatment inactivated TrxR1, induced accumulation of ROS and eventually resulted in oxidative stress-mediated apoptosis in CRC cells.

As both Trx and TrxR1 have been reported to be upregulated in numerous human cancer types, including leukemia, lung cancer, breast cancer and colorectal cancer among others, and be associated with increased tumor growth, drug resistance and poor patient prognosis, the thioredoxin

system has been recognized as an attractive target for anti-cancer drug development (4,6-10,40). This system plays a role in maintaining  $H_2O_2$  levels in cells via the conversion of  $H_2O_2$  to  $H_2O$ . Trx contains two adjacent thiols in its reduced form that are converted to a disulfide bond in the oxidized form (39). The oxidized Trx is then recycled back into the reduced form by TrxR1 and NADPH (35). The present study demonstrated that HT could significantly inhibit

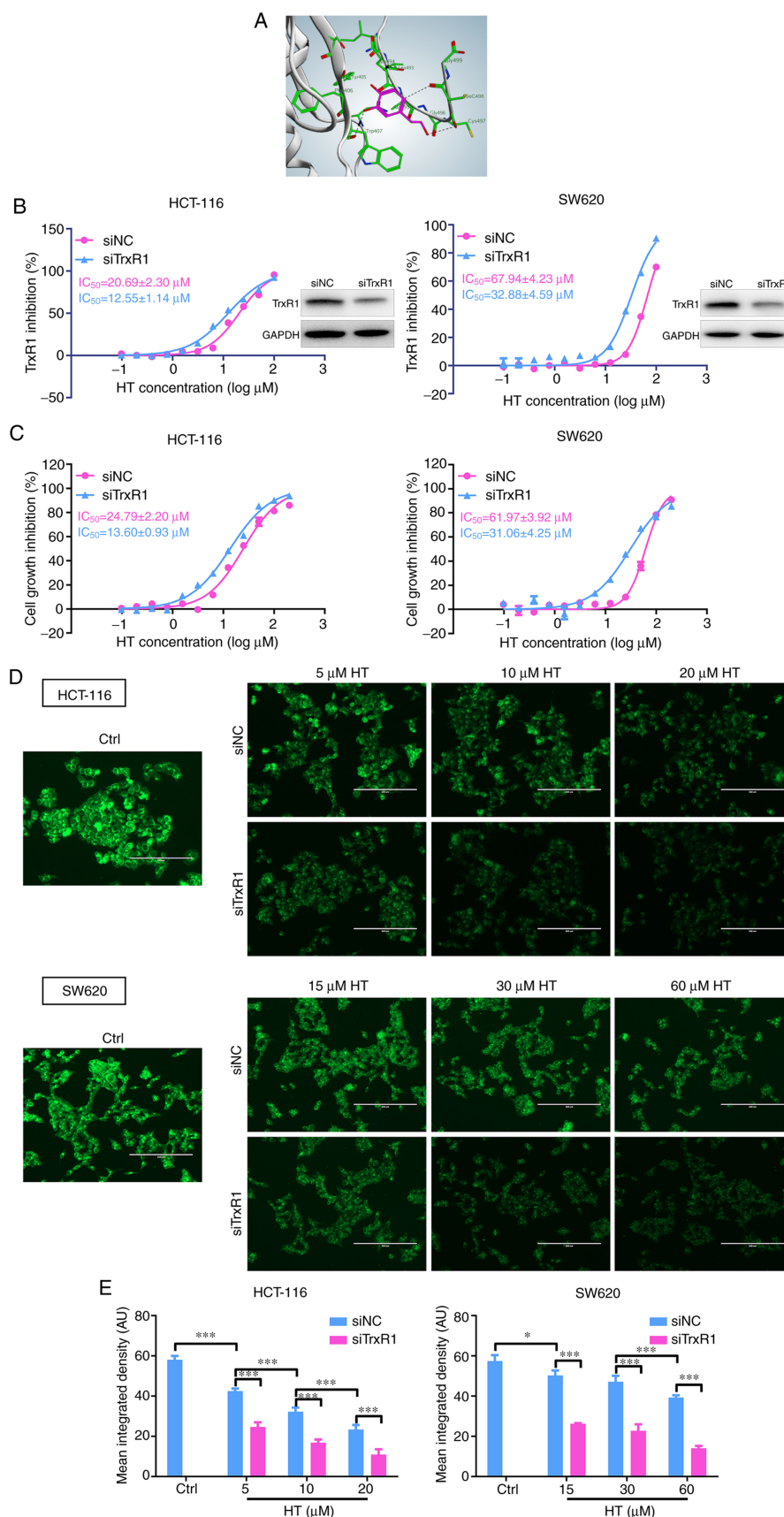


Figure 5. Cellular actions of HT are associated with its interaction with TrxR1. (A) Proposed binding mode of HT in the active site of TrxR1. TrxR1 residues are depicted in green and HT in purple. (B) Knockdown of TrxR1 expression attenuated the cellular enzyme inhibitory activity of HT in HCT-116 and SW620 cells. The enzyme activity of TrxR1 in HCT-116 and SW620 cells was measured via the endpoint insulin reduction assay. The expression of TrxR1 was analyzed via western blotting. (C) Antiproliferative effect of HT in siTrxR1 or siNC transfected cells. (D) Image-based TrxR1 activity assay in siRNA transfected HCT-116 and SW620 cells using the TRFS-green probe. siNC-treated cells were used as the negative controls. (E) Quantification of the mean fluorescence intensity in individual groups was performed. Scale bars, 200  $\mu\text{m}$ . \* $P<0.05$  and \*\*\* $P<0.005$ . si-, small interfering; TrxR1, thioredoxin reductase 1; HT, hydroxytyrosol; NC, negative control; AU, absorbance units.

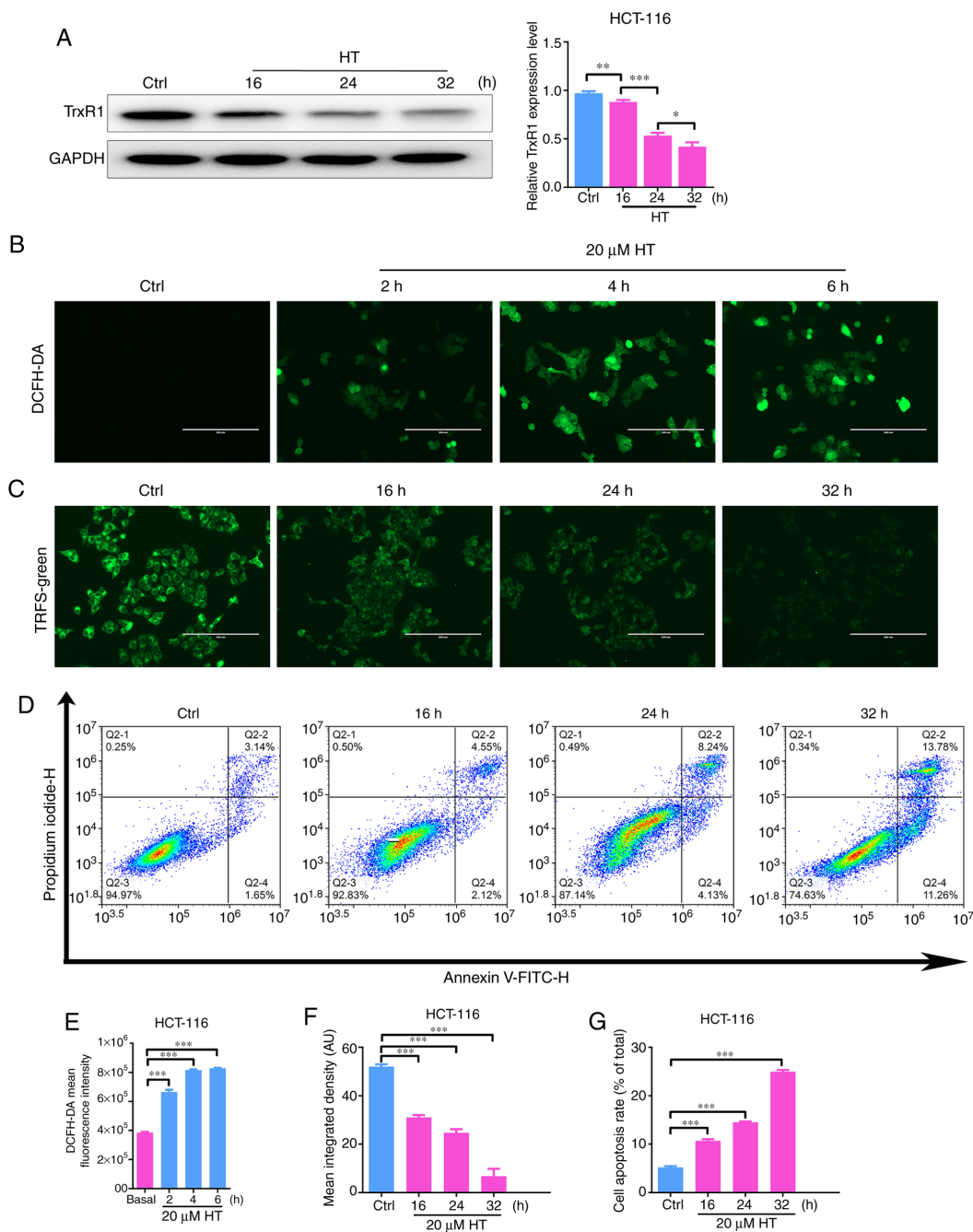


Figure 6. Time course assays of HT. HCT-116 cells were seeded overnight and then exposed to 20  $\mu$ M HT for the indicated time followed by time course assays. (A) Cell extracts were prepared and analyzed by western blotting with an antibody against TrxR1. TrxR1 levels were quantified and normalized to GAPDH. (B) Cells were stained with 10  $\mu$ M DCFH-DA and examined by fluorescence microscopy and flow cytometry. (C) Cells were incubated with the TrxR probe TRFS-green for 4 h, and fluorescence images were captured using fluorescence microscopy. (D) Cells were double stained by Annexin V/propidium iodide and analyzed by flow cytometry. (E) DCFH-DA mean fluorescence intensity was quantified by flow cytometry. (F) Quantification of the mean fluorescence intensity of TRFS-green in individual groups was performed. (G) The percentage of cell apoptosis was quantified and the cells in Q2-2 and Q2-4 were considered apoptotic. DMSO was used as the negative control. Scale bars, 200  $\mu$ m. \* $P$ <0.05, \*\* $P$ <0.01 and \*\*\* $P$ <0.005. TrxR1, thioredoxin reductase 1; HT, hydroxytyrosol; DCFH-DA, 2',7'-dichlorofluorescein diacetate; AU, absorbance units.

both recombinant and cellular TrxR1 enzyme activity. The mammalian TrxR1 enzyme uniformly harbors a critical Sec residue in its C-terminal active site. The high nucleophilicity of the Sec residue renders the enzyme vulnerable to be modified by electrophiles, based on which numerous selective TrxR1 inhibitors have been developed (4,5,40-44). The results of the current study revealed strong inhibition of the TrxR-wt enzyme but not the enzyme lacking the Sec residue (TrxR- $\Delta$ C), thus revealing the potential interaction

site between TrxR1 and HT. The docking results were also supportive of this hypothesis. Therefore, further investigation on HT could lead to the development of a novel strategy for treating CRC.

HT is a phenolic phytochemical with numerous medical properties (45). It is considered a chemopreventive agent due to its antioxidative properties (46). Recently, HT was indicated to be a promising anticancer compound. For instance, previous studies have demonstrated that HT can

induce oxidative stress in various cell lines, and the induction of ROS production is involved in the biological functions of HT (25,26,47-49). However, to the best of our knowledge, there is no detailed mechanism of how HT elevates oxidative stress. In the current study, TrxR1 was identified as a target of HT, and it was demonstrated that HT induced apoptosis and cell cycle arrest through a previously uncharacterized mechanism by targeting TrxR1. Binding of HT to TrxR1 inhibits the physiological functions of TrxR1, which leads to the conversion of H<sub>2</sub>O<sub>2</sub> to H<sub>2</sub>O and ROS accumulation within cells, and finally elicits oxidative stress. However, elevated TrxR1 activity has been observed in HT-treated PC12 cells (50), which indicated HT may exhibit a two-sided effect on ROS production. HT produces H<sub>2</sub>O<sub>2</sub> in the auto-oxidation process, which is a common event in cell culture media; however, different cell types exhibit various sensitivities to HT-induced H<sub>2</sub>O<sub>2</sub> and this leads to different cell fates (51). This depends on both the capability of cells to eliminate H<sub>2</sub>O<sub>2</sub> by specific enzymes, such as TrxR1, catalase and glutathione peroxidase, and the effectiveness by which HT releases H<sub>2</sub>O<sub>2</sub> in different cell culture media (52-54). Therefore, different concentrations of HT treatment in various cell types may lead to different levels of oxidative stress and, therefore, stimulate various effects of TrxR1. The cellular mechanisms by which HT exerts these effects are still poorly understood and require further elucidation.

To the best of our knowledge, there are no TrxR1 inhibitors used clinically to date. As a HT is novel TrxR1 inhibitor with a unique scaffold, it is difficult to select another inhibitor for comparison against HT. Therefore, a TrxR1 inhibitory experiment was performed to compare HT and the current most effective TrxR1 inhibitor, auranofin. Compared with the results of our previous study, auranofin exhibited better TrxR1 inhibitory activity compared with HT in HCT-116 cells (55). However, auranofin has insufficient physiological stability and this limits its clinical development (10). HT exhibited cellular enzyme inhibitory activity and inhibited proliferation of several colorectal cancer cells (HCT-116, SW620 and HCT-8) at the  $\mu$ mol levels, which demonstrated that it was an effective antitumor agent. Although its TrxR1 inhibitory activity is poor at present, its activity may be improved by further modification of its scaffold.

In conclusion, TrxR1 was investigated as a target of HT *in vitro* in human CRC cells, and it was demonstrated that HT induced oxidative stress-mediated apoptosis through a yet unclear mechanism. Furthermore, the results of the present study investigated the binding model between HT and TrxR1, which could serve as a new scaffold to develop novel TrxR1 inhibitors for CRC treatment.

#### Acknowledgements

Not applicable.

#### Funding

The present study was supported by Natural Science Foundation of Anhui Province (grant no. 1808085QH262), University Natural Science Research Project of Anhui Province (grant no. KJ2018A0259), Key Research and Development

Project of Anhui Province (grant no. 202004a07020041), Major University Natural Science Research Project of Anhui Province (grant no. KJ2019ZD30) and Foundation for Excellent Talents in Higher Education of Anhui Province (grant no. gxbjZD18).

#### Availability of data and materials

The datasets used and/or analyzed during the current study are available from the corresponding author on reasonable request.

#### Authors' contributions

SPZ and JZ performed the experiments, wrote the manuscript and analyzed the data. CZ and YMZ designed the experiments, wrote the manuscript and confirmed the authenticity of all the raw data. QZF and XML purified recombinant TrxR1 protein and performed TrxR1 enzyme activity assays. TW, FW, YC and SYH performed the apoptosis, cell cycle and western blotting assays. XPL performed the RNA interference assays. BSX and LH carried out the cell culture and treatment with the drug solutions. All authors have read and approved the final manuscript.

#### Ethics approval and consent to participate

Not applicable.

#### Patient consent for publication

Not applicable.

#### Competing interests

The authors declare that they have no competing interests.

#### References

1. Feng RM, Zong YN, Cao SM and Xu RH: Current cancer situation in China: Good or bad news from the 2018 global cancer statistics? *Cancer Commun (Lond)* 39: 22, 2019.
2. Lucas C, Barnich N and Nguyen HT: Microbiota, inflammation and colorectal cancer. *Int J Mol Sci* 18: 1310, 2017.
3. Wang X and Li T: Development of a 15-gene signature for predicting prognosis in advanced colorectal cancer. *Bioengineered* 11: 165-174, 2020.
4. Bian M, Wang X, Sun Y and Liu W: Synthesis and biological evaluation of gold(III) Schiff base complexes for the treatment of hepatocellular carcinoma through attenuating TrxR activity. *Eur J Med Chem* 193: 112234, 2020.
5. Yao J, Duan D, Song ZL, Zhang J and Fang J: Sanguinarine as a new chemical entity of thioredoxin reductase inhibitor to elicit oxidative stress and promote tumor cell apoptosis. *Free Radic Biol Med* 20: 659-667, 2020.
6. Kim SJ, Miyoshi Y, Taguchi T, Tamaki Y, Nakamura H, Yodoi J, Kato K and Noguchi S: High thioredoxin expression is associated with resistance to docetaxel in primary breast cancer. *Clin Cancer Res* 11: 8425-8430, 2005.
7. Peng W, Zhou Z, Zhong Y, Sun Y, Wang Y, Zhu Z, Jiao W, Bai M, Sun J, Lu J and Yin H: Plasma activity of thioredoxin reductase as a novel biomarker in gastric cancer. *Sci Rep* 9: 19084, 2019.
8. Xu L, Zhao Y, Pan F, Zhu M, Yao L, Liu Y, Feng J, Xiong J, Chen X, Ren F, *et al*: Inhibition of the Nrf2-TrxR axis sensitizes the drug-resistant chronic myelogenous leukemia cell line K562/G01 to imatinib treatments. *Biomed Res Int* 2019: 6502793, 2019.

9. Zhu B, Ren C, Du K, Zhu H, Ai Y, Kang F, Luo Y, Liu W, Wang L, Xu Y, *et al*: Oleic acid plays a role in cisplatin-mediated apoptosis and reverses cisplatin resistance in human lung cancer through multiple signaling pathways. *Biochem Pharmacol* 170: 113642, 2019.
10. Bian M, Fan R, Zhao S and Liu W: Targeting the thioredoxin system as a strategy for cancer therapy. *J Med Chem* 62: 7309-7321, 2019.
11. Zhang J, Li X, Han X, Liu R and Fang J: Targeting the thioredoxin system for cancer therapy. *Trends Pharmacol Sci* 38: 794-808, 2017.
12. Arnér ES: Targeting the selenoprotein thioredoxin reductase 1 for anticancer therapy. *Adv Cancer Res* 136: 139-151, 2017.
13. Scalcon V, Bindoli A and Rigobello MP: Significance of the mitochondrial thioredoxin reductase in cancer cells: An update on role, targets and inhibitors. *Free Radic Biol Med* 127: 62-79, 2018.
14. Stafford WC, Peng X, Olofsson MH, Zhang X, Luci DK, Lu L, Cheng Q, Trésaugues L, Dexheimer TS, Coussens NP, *et al*: Irreversible inhibition of cytosolic thioredoxin reductase 1 as a mechanistic basis for anticancer therapy. *Sci Transl Med* 10: eaaf7444, 2018.
15. Kingston DG: Modern natural products drug discovery and its relevance to biodiversity conservation. *J Nat Prod* 74: 496-511, 2011.
16. Mishra BB and Tiwari VK: Natural products: An evolving role in future drug discovery. *Eur J Med Chem* 46: 4769-4807, 2011.
17. Stefanon B and Colitti M: Original research: Hydroxytyrosol, an ingredient of olive oil, reduces triglyceride accumulation and promotes lipolysis in human primary visceral adipocytes during differentiation. *Exp Biol Med* 241: 1796-1802, 2016.
18. Goldstein DS, Jinsmaa Y, Sullivan P, Holmes C, Kopin IJ and Sharabi Y: 3,4-dihydroxyphenylethanol (hydroxytyrosol) mitigates the increase in spontaneous oxidation of dopamine during monoamine oxidase inhibition in PC12 cells. *Neurochem Res* 41: 2173-2178, 2016.
19. Persia FA, Mariani ML, Fogal TH and Penissi AB: Hydroxytyrosol and oleuropein of olive oil inhibit mast cell degranulation induced by immune and non-immune pathways. *Phytomedicine* 21: 1400-1405, 2014.
20. Bedoya LM, Beltrán M, Obregón-Calderón P, García-Pérez J, de la Torre HE, González N, Pérez-Olmeda M, Auñón D, Capa L, Gómez-Acebo E and Alcamí J: Hydroxytyrosol: A new class of microbicide displaying broad anti-HIV-1 activity. *AIDS* 30: 2767-2776, 2016.
21. Walter WM Jr, Fleming HP and Etchells JL: Preparation of antimicrobial compounds by hydrolysis of oleuropein from green olives. *Appl Microbiol* 26: 773-776, 1973.
22. Medina E, de Castro A, Romero C and Brenes M: Comparison of the concentrations of phenolic compounds in olive oils and other plant oils: Correlation with antimicrobial activity. *J Agric Food Chem* 54: 4954-4961, 2006.
23. Sirianni R, Chimento A, De Luca A, Casaburi I, Rizza P, Onofrio A, Iacopetta D, Puoci F, Andò S, Maggiolini M and Pezzi V: Oleuropein and hydroxytyrosol inhibit MCF-7 breast cancer cell proliferation interfering with ERK1/2 activation. *Mol Nutr Food Res* 54: 833-840, 2010.
24. Chimento A, Casaburi I, Rosano C, Avena P, De Luca A, Campana C, Martire E, Santolla MF, Maggiolini M, Pezzi V and Sirianni R: Oleuropein and hydroxytyrosol activate GPER/GPR30-dependent pathways leading to apoptosis of ER-negative SKBR3 breast cancer cells. *Mol Nutr Food Res* 58: 478-489, 2014.
25. Luo C, Li Y, Wang H, Cui Y, Feng Z, Li H, Li Y, Wang Y, Wurtz K, Weber P, *et al*: Hydroxytyrosol promotes superoxide production and defects in autophagy leading to anti-proliferation and apoptosis on human prostate cancer cells. *Curr Cancer Drug Targets* 13: 625-639, 2013.
26. Sun L, Luo C and Liu J: Hydroxytyrosol induces apoptosis in human colon cancer cells through ROS generation. *Food Funct* 5: 1909-1914, 2014.
27. Totoda G, Lupinacci S, Vizza D, Bonfiglio R, Perri E, Bonfiglio M, Lofaro D, La Russa A, Leone F, Gigliotti P, *et al*: High doses of hydroxytyrosol induce apoptosis in papillary and follicular thyroid cancer cells. *J Endocrinol Invest* 40: 153-162, 2017.
28. Terzuoli E, Giachetti A, Ziche M and Donnini S: Hydroxytyrosol, a product from olive oil, reduces colon cancer growth by enhancing epidermal growth factor receptor degradation. *Mol Nutr Food Res* 60: 519-529, 2016.
29. Zhao B, Ma Y, Xu Z, Wang J, Wang F, Wang D, Pan S, Wu Y, Pan H, Xu D, *et al*: Hydroxytyrosol, a natural molecule from olive oil, suppresses the growth of human hepatocellular carcinoma cells via inactivating AKT and nuclear factor-kappa B pathways. *Cancer Lett* 347: 79-87, 2014.
30. Zubair H, Bhardwaj A, Ahmad A, Srivastava SK, Khan MA, Patel GK, Singh S and Singh AP: Hydroxytyrosol induces apoptosis and cell cycle arrest and suppresses multiple oncogenic signaling pathways in prostate cancer cells. *Nutr Cancer* 69: 932-942, 2017.
31. Zhang J, Zhang B, Li X, Han X, Liu R and Fang J: Small molecule inhibitors of mammalian thioredoxin reductase as potential anticancer agents: An update. *Med Res Rev* 39: 5-39, 2019.
32. Arnér ES, Sarioglu H, Lottspeich F, Holmgren A and Böck A: High-level expression in *Escherichia coli* of selenocysteine-containing rat thioredoxin reductase utilizing gene fusions with engineered bacterial-type SECIS elements and co-expression with the selA, selB and selC genes. *J Mol Biol* 292: 1003-1016, 1999.
33. Zhang L, Duan D, Liu Y, Ge C, Cui X, Sun J and Fang J: Highly selective off-on fluorescent probe for imaging thioredoxin reductase in living cells. *J Am Chem Soc* 136: 226-233, 2014.
34. Zhang J, Duan D, Osama A and Fang J: Natural molecules targeting thioredoxin system and their therapeutic potential. *Antioxid Redox Signal* 34: 1083-1107, 2021.
35. Zhang J, Duan D, Song ZL, Liu T, Hou Y and Fang J: Small molecules regulating reactive oxygen species homeostasis for cancer therapy. *Med Res Rev* 41: 342-394, 2021.
36. Zhong L and Holmgren A: Essential role of selenium in the catalytic activities of mammalian thioredoxin reductase revealed by characterization of recombinant enzymes with selenocysteine mutations. *J Biol Chem* 275: 18121-18128, 2000.
37. Zhong L, Arnér ES and Holmgren A: Structure and mechanism of mammalian thioredoxin reductase: The active site is a redox-active selenolthiol/selenenylsulfide formed from the conserved cysteine-selenocysteine sequence. *Proc Natl Acad Sci U S A* 97: 5854-5859, 2000.
38. Cai W, Zhang L, Song Y, Wang B, Zhang B, Cui X, Hu G, Liu Y, Wu J and Fang J: Small molecule inhibitors of mammalian thioredoxin reductase. *Free Radic Biol Med* 52: 257-265, 2012.
39. Lo YC, Ko TP, Su WC, Su TL and Wang AH: Terpyridine-platinum(II) complexes are effective inhibitors of mammalian topoisomerases and human thioredoxin reductase 1. *J Inorg Biochem* 103: 1082-1092, 2009.
40. Ng HL, Ma X, Chew EH and Chui WK: Design, synthesis, and biological evaluation of coupled bioactive scaffolds as potential anticancer agents for dual targeting of dihydrofolate reductase and thioredoxin reductase. *J Med Chem* 60: 1734-1745, 2017.
41. Liu Y, Duan D, Yao J, Zhang B, Peng S, Ma H, Song Y and Fang J: Dithiaarsanes induce oxidative stress-mediated apoptosis in HL-60 cells by selectively targeting thioredoxin reductase. *J Med Chem* 57: 5203-5211, 2014.
42. Zhang B, Duan D, Ge C, Yao J, Liu Y, Li X and Fang J: Synthesis of xanthohumol analogues and discovery of potent thioredoxin reductase inhibitor as potential anticancer agent. *J Med Chem* 58: 1795-1805, 2015.
43. Tuladhar A and Rein KS: Manumycin A is a potent inhibitor of mammalian thioredoxin reductase-1 (TrxR-1). *ACS Med Chem Lett* 9: 318-322, 2018.
44. Xie L, Luo Z, Zhao Z and Chen T: Anticancer and antiangiogenic iron(II) complexes that target thioredoxin reductase to trigger cancer cell apoptosis. *J Med Chem* 60: 202-214, 2017.
45. Bertelli M, Kiani AK, Paolacci S, Manara E, Kurti D, Dhuli K, Bushati V, Miertus J, Pangallo D, Baglivo M, *et al*: Hydroxytyrosol: A natural compound with promising pharmacological activities. *J Biotechnol* 309: 29-33, 2020.
46. Britton J, Davis R and O'Connor KE: Chemical, physical and biotechnological approaches to the production of the potent antioxidant hydroxytyrosol. *Appl Microbiol Biotechnol* 103: 5957-5974, 2019.
47. Romana-Souza B, Saguie BO, Pereira de Almeida Nogueira N, Paes M, Dos Santos Valença S, Atella GC and Monte-Alto-Costa A: Oleic acid and hydroxytyrosol present in olive oil promote ROS and inflammatory response in normal cultures of murine dermal fibroblasts through the NF- $\kappa$ B and NRF2 pathways. *Food Res Int* 131: 108984, 2020.
48. Sun T, Chen Q, Zhu SY, Wu Q, Liao CR, Wang Z, Wu XH, Wu HT and Chen JT: Hydroxytyrosol promotes autophagy by regulating SIRT1 against advanced oxidation protein product-induced NADPH oxidase and inflammatory response. *Int J Mol Med* 44: 1531-1540, 2019.

49. Avola R, Graziano AC, Pannuzzo G, Bonina F and Cardile V: Hydroxytyrosol from olive fruits prevents blue-light-induced damage in human keratinocytes and fibroblasts. *J Cell Physiol* 234: 9065-9076, 2019.
50. Peng S, Zhang B, Yao J, Duan D and Fang J: Dual protection of hydroxytyrosol, an olive oil polyphenol, against oxidative damage in PC12 cells. *Food Funct* 6: 2091-2100, 2015.
51. Long LH, Hoi A and Halliwell B: Instability of, and generation of hydrogen peroxide by, phenolic compounds in cell culture media. *Arch Biochem Biophys* 501: 162-169, 2010.
52. Fabiani R, Fuccelli R, Pieravanti F, De Bartolomeo A and Morozzi G: Production of hydrogen peroxide is responsible for the induction of apoptosis by hydroxytyrosol on HL60 cells. *Mol Nutr Food Res* 53: 887-896, 2009.
53. Fabiani R, Sepporta MV, Rosignoli P, De Bartolomeo A, Crescimanno M and Morozzi G: Anti-proliferative and pro-apoptotic activities of hydroxytyrosol on different tumour cells: The role of extracellular production of hydrogen peroxide. *Eur J Nutr* 51: 455-464, 2012.
54. Rosignoli P, Fuccelli R, Sepporta MV and Fabiani R: In vitro chemo-preventive activities of hydroxytyrosol: The main phenolic compound present in extra-virgin olive oil. *Food Funct* 7: 301-307, 2016.
55. Fan QZ, Zhou J, Zhu YB, He LJ, Miao DD, Zhang SP, Liu XP and Zhang C: Design, synthesis, and biological evaluation of a novel indoleamine 2,3-dioxygenase 1 (IDO1) and thioredoxin reductase (TrxR) dual inhibitor. *Bioorg Chem* 105: 104401, 2020.



This work is licensed under a Creative Commons Attribution-NonCommercial-NoDerivatives 4.0 International (CC BY-NC-ND 4.0) License.